Silencing the Hydroxyproline-Rich Glycopeptide Systemin Precursor in Two Accessions of *Nicotiana attenuata* Alters Flower Morphology and Rates of Self-Pollination[1][W][OA]

Beatrice Berger and Ian T. Baldwin*

Department of Molecular Ecology, Max-Planck-Institute for Chemical Ecology, D–07745 Jena, Germany

Systemins and their hydroxyproline-rich glycopeptide systemin (ppHS) subfamily members are known to mediate antiherbivore defenses in some solanaceous taxa but not others; functions other than in defense remain largely unexplored. *Nicotiana attenuata*'s ppHS is known not to function in herbivore defense. *NappHS* transcripts are abundant in flowers, particularly in pistils, and when two *N. attenuata* accessions from Utah and Arizona were transformed to silence *NappHS* by RNAi (IRsys), seed capsule production and seed number per capsule were reduced in both accessions. These reductions in reproductive performance could not be attributed to impaired pollen or ovule viability; hand-pollination of all IRsys lines of both accessions restored seed production per capsule to levels found in wild-type plants. Rather, changes in flower morphology that decreased the efficiency of self-pollination are likely responsible: IRsys plants of both accessions have flowers with pistils that protrude beyond their anthers. Because these changes in flower morphology are reminiscent of *CORONATINE-INSENSITIVE1*-silenced *N. attenuata* plants, we measured jasmonates (JAs) and their biosynthetic transcripts in different floral developmental stages, and found levels of JA-isoleucine (Ile)/leucine and threonine deaminase transcripts, which are abundant in wild-type pistils, to be significantly reduced in IRsys buds and flowers. Threonine deaminase supplies Ile for JA-Ile biosynthesis, and we propose that ppHS mediates JA signaling during flower development and thereby changes flower morphology. These results suggest that the function of *ppHS* family members in *N. attenuata* may have diversified to modulate flower morphology and thereby outcrossing rates in response to biotic or abiotic stresses.

Signaling peptides that activate plant defense genes are defined as members of the systemin family (Pearce and Ryan, 2003); until now, however, no common mode of action has been uncovered. While the systemin peptide in tomato (*Solanum lycopersicum*) amplifies a jasmonate (JA)-based signal to activate the antidigestive trypsin proteinase inhibitor (TPI) and other defensive genes (Schilmiller and Howe, 2005), its homolog in black nightshade (*Solanum nigrum*) is not involved in TPI's production (Schmidt and Baldwin, 2006), but, rather, appears to help the plant tolerate rather than resist herbivory (Schmidt and Baldwin, 2009). Hyp-rich glycopeptides (HypSys) purified from cultivated tobacco (*Nicotiana tabacum*) are members of a systemin subfamily; recently they were reported to act as defense signals in cultivated tobacco. The 164-amino acid precursor that encodes the two tobacco peptides has no sequence homology with the 200-amino acid systemin tomato precursor. The two mature HypSys peptides from tobacco share a weak amino acid homology to the tomato systemin. Moreover, the -PPS- motif found in tomato systemin is modified to -OOS- and the Hyp residues are posttranslationally modified with pentose glycosylations (Pearce et al., 2001). The hydroxylation of the Pro residues, the carbohydrate decorations, and a leader sequence indicate that tobacco HypSys peptides are synthesized through the secretory system, unlike tomato systemin, which has none of these features (McGurl et al., 1992; Pearce et al., 2001). These modifications increase the technical challenges of characterizing and synthesizing the HypSys peptides and likely add another level of specificity to their potential function.

HypSys peptides isolated from attacked tobacco leaves were shown to elicit the tobacco trypsin inhibitor, a paralog of the tomato protease inhibitor II, when applied to the cut petioles of tobacco leaves (Pearce et al., 2001). HypSys peptides involved in antiherbivore defense signaling were, however, also found in tomato (Pearce and Ryan, 2003) and may regulate systemic wound signaling as well as systemin in tomato (Narváez-Vásquez et al., 2007). Whereas Hyp-

[1] This work was supported by the Max Planck Society.

* Corresponding author; e-mail baldwin@ice.mpg.de.

The author responsible for the distribution of materials integral to the findings presented in this article in accordance with the policy described in the Instructions for Authors (www.plantphysiol.org) is: Ian T. Baldwin (baldwin@ice.mpg.de).

[W] The online version of this article contains Web-only data.

[OA] Open access articles can be viewed online without a subscription.

www.plantphysiol.org/cgi/doi/10.1104/pp.108.132928

Sys peptides in cultivated tobacco and tomato were found to mediate antiherbivore defense signaling, HypSys peptides purified from petunia (*Petunia hybrida*) did not. Although they were found to activate *defensin1*, a gene associated with antipathogen defense, they were not able to induce antiherbivore protease inhibitor or polyphenol oxidase activity (Pearce et al., 2007). This variability in function within the systemin gene family as well as within the HypSys systemin subfamily argues against a commonly conserved function.

Nicotiana attenuata, a wild diploid tobacco, is native to the southwestern deserts of the United States, with populations across Utah, Arizona, and California. The plant is self compatible, and is known to exhibit adaptive morphological and chemical phenotypic plasticity in response to biotic and abiotic factors, including the JA-mediated production of defense metabolites such as nicotine or TPIs in response to herbivore attack (Baldwin, 2001). Two morphologically similar *N. attenuata* accessions, Arizona (AZ) and Utah (UT), differ in their responses to insect herbivore attack. Plants of the AZ accession do not produce TPIs due to a nonsense mutation in the *pi* gene (Glawe et al., 2003; Wu et al., 2006). AZ plants' reproductive performance is higher than that of UT, as evidenced by an increase in the number of seed capsules when AZ plants are grown in competition with UT plants. The loss in fitness has been shown to be directly attributable to production of TPIs (Glawe et al., 2003; Zavala et al., 2004).

N. attenuata contains a homolog of the Hyp-rich systemin glycopeptide precursor found in cultivated tobacco. But *N. attenuata* plants of the UT accession that were silenced for their ability to express the HypSys precursor gene (*NappHS*) by RNAi did not differ from wild-type plants in their ability to produce TPIs or other JA-mediated antiherbivore defenses (Berger and Baldwin, 2007). This work ruled out a central role for *NappHS* in the JA-mediated antiherbivore defense responses of *N. attenuata* UT. The Hyp-rich systemin glycopeptide genes may evolve rapidly, perhaps even attaining new functions, as suggested by the findings in cultivated tobacco and petunia. Hence, it is possible that while the UT accession does not rely on ppHS for its antiherbivore defenses, other *N. attenuata* accessions might. To test this hypothesis, we transformed the AZ accession with an RNAi construct to silence *NappHS* transcript accumulation and evaluated defense-related attributes. Again we found no evidence that *NappHS* functions in the JA-mediated antiherbivore defense responses, similar to what we had found for plants of the UT accession. Hence, the question remains: Does ppHS function as a signal peptide in *N. attenuata* and if so what functions does it mediate? *NappHS* transcripts are particularly abundant in flowers (Berger and Baldwin, 2007) and here we turn our attention to functions that this peptide might be playing in reproductive organs.

RESULTS

PpHS Does Not Mediate Antiherbivore Defense Responses in AZ Plants

We expanded our previous analysis of *NappHS*'s role in mediating *N. attenuata*'s antiherbivore responses to plants of the AZ accession. We detected no change in *NappHS* transcripts in leaves treated with oral secretions of *Manduca sexta* or systemic leaves, AZ wild-type plants (Supplemental Fig. S1A). We generated two independently transformed lines each harboring a single insertion of the transformation vector (Supplemental Fig. S1B) and confirmed the reduction in ppHS transcripts by real-time quantitative (q)PCR analysis (Supplemental Fig. S1C), and that they were diploid by flow cytometry. IRsys lines contained only 1.2% of the ppHS transcripts of AZ wild-type plants. Interestingly, the transformed plants, with low endogenous ppHS levels, contained the same amount of nicotine as nontransformed plants (Supplemental Fig. S1D; ANOVA, $F_{2,9} = 0.414$, $P > 0.45$) and they were not impaired in the wound-induced increase in nicotine accumulation (Supplemental Fig. S1D; ANOVA, $F_{2,12} = 1.925$, $P > 0.0812$). Similar observations were found in ppHS-silenced plants of the UT accession (Berger and Baldwin, 2007).

Growth and Flowering

To examine whether the *NappHS* gene influences the growth performance of *N. attenuata*, we measured stalk lengths of AZ and UT accessions and their respective silenced lines and found no significant difference between wild-type and IRsys lines (AZ, Supplemental Fig. S2A, left section; ANOVA, Bonferroni-corrected post-hoc test, $F_{2,26} = 2.585$, $P > 0.05$; UT, Supplemental Fig. S2A, right section; ANOVA, Bonferroni-corrected post-hoc test, $F_{2,27} = 0.047$, $P > 0.05$). Only plants from AZ IRsys line 2 differed in their stalk lengths from AZ wild-type plants on days 4 (ANOVA, Bonferroni-corrected post-hoc test, $F_{2,26} = 4.424$, $P = 0.0133$) and 6 (ANOVA, Bonferroni-corrected post-hoc test, $F_{2,26} = 5.375$, $P = 0.0033$).

Plants of the AZ IRsys and UT IRsys lines did not differ significantly in the timing of the appearance of the first flowers, compared to their respective wild-type (AZ, Supplemental Fig. S2A, arrows; ANOVA, Bonferroni-corrected post-hoc test, $F_{2,27} = 5.424$, $P > 0.05$; UT, Supplemental Fig. S2A, arrows; ANOVA, Bonferroni-corrected post-hoc test, $F_{2,27} = 3.580$, $P > 0.05$) plants. In addition, the number of flowers per plant in AZ wild-type and IRsys lines was the same (Supplemental Fig. S2B, left section; ANOVA, Bonferroni-corrected post-hoc test, $F_{2,26} = 0.118$, $P > 0.05$); this was also true for the UT accession (Supplemental Fig. S2B, right section; ANOVA, Bonferroni-corrected post-hoc test, $F_{2,27} = 3.022$, $P > 0.05$). Reductions in aboveground biomass were correlated with low endogenous *NappHS* levels in AZ (Supplemental Fig. S2C, left section; ANOVA, Bonferroni-corrected post-hoc test,

$F_{2,45}$ = 10.037, $P \leq 0.0061$) and in UT IRsys line 2 (Supplemental Fig. S2C, right section; ANOVA, Bonferroni-corrected post-hoc test, $F_{2,37}$ = 23.658, $P < 0.0001$), but not in UT IRsys line 1.

Silencing *NappHS* Reduces the Number of Seed Capsules Produced in Both UT and AZ Accessions

A plant's reproductive success and therefore its fitness are strongly correlated with its seed capsule production. To determine whether silencing the *NappHS* gene has fitness consequences for *N. attenuata*, we counted the number of seed capsules per plant. We found conspicuously lower numbers of seed capsules in *NappHS*-silenced lines of both accessions compared to their respective wild type: AZ (Fig. 1A, top, left section; ANOVA, Bonferroni-corrected post-hoc test, $F_{2,52}$ = 92.379, $P < 0.0001$) and UT (Fig. 1A, top, right section; ANOVA, Bonferroni-corrected post-hoc test, $F_{2,39}$ = 16.403, $P \leq 0.0009$). Consistent with the results from Glawe et al. (2003), the number of seed capsules in AZ plants was higher than in UT plants. Since a plant's fitness is largely determined by the product of the number of seed capsules times the number of seeds per capsule, we counted the number of seeds per capsule in the first four to five ripened capsules per plant. IRsys lines of UT plants had slightly fewer seeds per capsule than UT wild-type plants (Fig. 1A, bottom, right section; ANOVA, Bonferroni-corrected post-hoc test, $F_{2,61}$ = 1.681, $P > 0.05$), and in AZ, significant differences were detected between IRsys and wild-type plants (Fig. 1A, bottom, left section; ANOVA, Bonferroni-corrected post-hoc test, $F_{2,64}$ = 5.920, $P \leq 0.0126$).

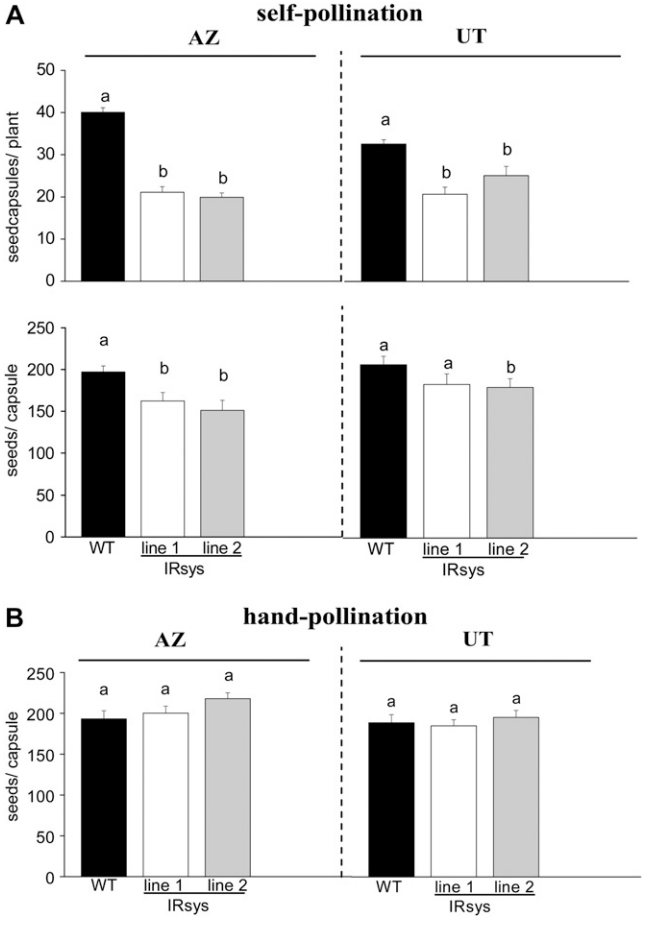

Figure 1. Silencing *NappHS* reduces the number of seed capsules produced in two accessions of *N. attenuata*. Mean ± SE number of mature seed capsules of 12 to 15 (A, top) wild-type (WT, black bars), IRsys line 1 (white bars), and IRsys line 2 (gray bars) plants of the AZ (left section) and UT (right section) accessions. Mean ± SE seed number per capsule of the first four to five ripe self-pollinated capsules per plant (n = 12) of each genotype (A) and of emasculated and hand-pollinated flowers (B). Different letters indicate significant differences from wild-type plants as determined by ANOVA followed by Bonferroni-corrected post-hoc test.

To determine if low seed numbers per capsule were due to deficiencies in pollen or ovule viability, we emasculated flowers and pollinated them by hand with pollen of the respective genotype. Hand-pollination restored seed production of IRsys plants to wild-type levels in both accessions: AZ (Fig. 1B, left section; ANOVA, Bonferroni-corrected post-hoc test, $F_{2,29}$ = 2.338, $P > 0.05$) and UT (Fig. 1B, right section; ANOVA, Bonferroni-corrected post-hoc test, $F_{2,23}$ = 0.7180, $P > 0.05$). We also examined the viability of the pollen by staining it with fluorescine diacetate and found no differences in pollen viability among any of the genotypes (Supplemental Fig. S3).

Silencing *NappHS* Is Associated with Elongated Pistils in *N. attenuata* Flowers

Since reduced seed capsule and seed numbers in IRsys plants of both accessions was not due to reduced flower numbers or nonviable pollen or ovules, the differences may simply be the result of pollen limitation, which was equalized when emasculated flowers were hand-pollinated. We observed that IRsys plants silenced in *NappHS* produce flowers with stigmas that protruded beyond the stamen (Fig. 2A). In contrast, in wild-type flowers of both accessions, the stigma is almost in the same plane as the stamen when the flower opens and the anthers dehisce, or even below it. Approximately 90% of the flowers in *NappHS*-silenced lines showed an elongated stigma, whereas only 24% (AZ) and 26% (UT) of the wild-type plants did (Supplemental Fig. S4; ANOVA, Bonferroni-corrected post-hoc test, $P < 0.0001$).

We found significant differences in the IRsys flowers of both accessions when measuring the distance between the stigma and the anther of the longest filament (Fig. 2C; ANOVA, Bonferroni-corrected post-hoc test, $P < 0.0001$). In contrast, the stigma of wild-type flowers was on the same level or below the anther of the longest filament in AZ flowers (wild type: −0.120 ± 0.025 mm; IRsys line 1: 0.145 ± 0.015 mm; IRsys line 2: 0.096 ± 0.020 mm) and in UT flowers (wild type: −0.062 ± 0.017 mm; IRsys line 1: 0.128 ± 0.015 mm;

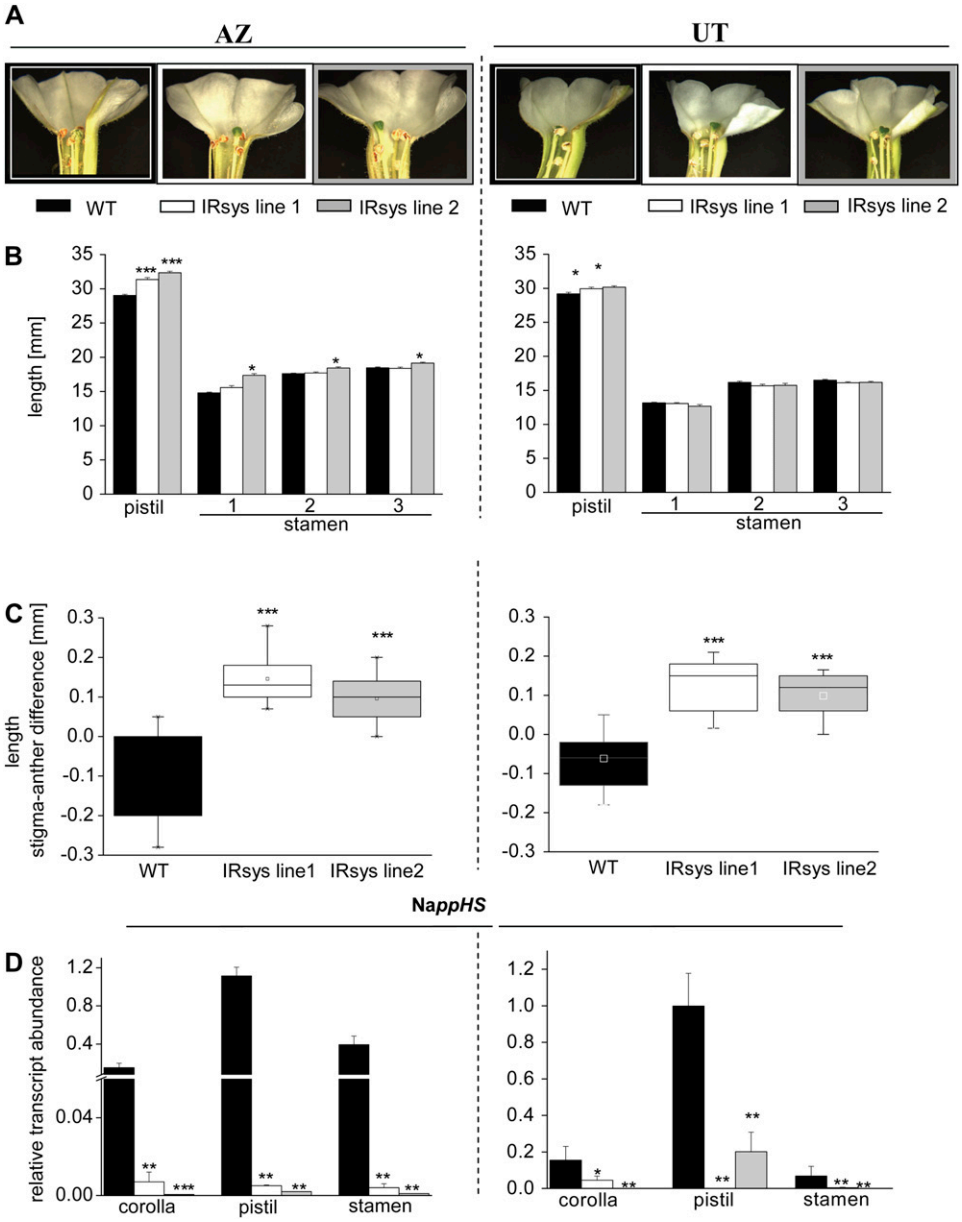

Figure 2. Silencing *NappHS* is associated with elongated pistils in *N. attenuata* flowers. A, Characteristic morphology of fully opened flowers of AZ wild type (WT), AZ IRsys line 1, and AZ IRsys line 2 (left section) plants, and of UT wild type, UT IRsys line 1, and UT IRsys line 2 (right section) plants. B, Mean ± SE pistil and stamen lengths (mm) of 12 flowers per genotype. Stamen 1 is the shortest, 2 the middle length, and 3 the longest stamen of the flower. C, Differences in length (mm) between the stigma and the anther of the longest filament of 10 to 24 fully opened flowers of each genotype. D, Relative transcript abundance of *NappHS* in corolla, pistil, and stamens of three to five replicate wild-type (black bars), IRsys line 1 (white bars), and IRsys line 2 (gray bars) plants of AZ (left section) and UT (right section) accessions. Asterisks indicate significant differences (*** < 0.001, ** < 0.005, * < 0.05); ANOVA followed by Bonferroni-corrected post-hoc test.

IRsys line 2: 0.099 ± 0.014 mm). As this difference could be due to either elongation of the stigma or shortening of the filaments, we measured the total length of pistil and stamen in all genotypes. We found longer pistils in the silenced lines of both accessions AZ (Fig. 2B, left section; ANOVA, Bonferroni-corrected post-hoc test, $F_{2,33} = 53.519$, $P < 0.0001$) and UT (Fig. 2B, right section; ANOVA, Bonferroni-corrected post-hoc test, $F_{2,30} = 5.035$, $P \leq 0.0109$) compared to their respective wild type. Stamens were not significantly shorter from wild type in either ppHS-silenced line (Fig. 2C, right section; ANOVA, Bonferroni-corrected post-hoc test, $P > 0.05$). Finally, we found significantly longer stamens in the AZ IRsys line 2 (Fig. 2C, left section; ANOVA, Bonferroni-corrected post-hoc test, $P \leq 0.0036$).

Interestingly, pistils of both accessions had the highest abundance of *NappHS* transcripts compared to stamens and corollas (Fig. 2D, left and right sections) of the same flower. As Figure 2D demonstrates, *NappHS* transcripts were significantly reduced in all flower parts of all transformed lines.

NappHS-Silenced Buds and Flowers Accumulate Lower Levels of JAs

Many developmental processes are described to be orchestrated by JAs. Since there is evidence that the tomato systemin peptide is involved in amplifying a JA-based mobile wound signal, the question arose: Is the flower phenotype in the IRsys lines also mediated by JAs? To address this question, we measured the JA

and JA-Ile/Leu concentration in three different developmental stages of the flowers. All developmental stages of IRsys flowers contained less JA-Ile/Leu than their respective wild types (Fig. 3, A–C). This was true for three developmental stages of reproductive meristems: small buds (5–10 mm) of AZ IRsys lines (Fig. 3A, left section; ANOVA, Bonferroni-corrected post-hoc test, $F_{2,12} = 9.975$, $P \leq 0.0026$) and of UT IRsys lines (Fig. 3A, right section; ANOVA, genotype, Bonferroni-corrected post-hoc test, $F_{2,12} = 21.718$, $P \leq 0.0035$), buds (30–40 mm; Fig. 3B, AZ IRsys lines; ANOVA, Bonferroni-corrected post-hoc test, $F_{2,14} = 15.731$, $P \leq 0.0003$; and UT IRsys lines; ANOVA, Bonferroni-corrected post-hoc test, $F_{2,12} = 21.718$, $P \leq 0.0035$), and flowers (Fig. 3C, AZ IRsys lines; ANOVA, Bonferroni-corrected post-hoc test, $F_{2,14} = 15.731$, $P \leq 0.0003$; and UT IRsys lines; ANOVA, Bonferroni-corrected post-hoc test, $F_{2,14} = 20.260$, $P \leq 0.0003$). JA-Ile/Leu contents in AZ and UT plants decreased throughout flower formation, with the lowest JA-Ile/Leu values in fully opened flowers. This was also found in the ppHS-silenced lines as well (Fig. 3C).

JA contents decreased even more drastically. Whereas small amounts were detectable in small buds (1,000 ng g^{-1} fresh mass in AZ and 800 ng g^{-1} fresh mass in UT; Fig. 3D), fully opened flowers contained only minute amounts of JA (Fig. 3F). The JA content of bud and flower tissue in all the transgenic lines was significantly lower than that of the bud and flower tissue in UT wild-type plants: small buds (Fig. 3D, right section; ANOVA, Bonferroni-corrected post-hoc test, $F_{2,12} = 13.589$, $P \leq 0.0030$), older buds (Fig. 3E, right section; ANOVA, Bonferroni-corrected post-hoc test, $F_{2,14} = 6.769$, $P \leq 0.0063$), and flowers (Fig. 3F, right section; ANOVA, $F_{2,12} = 6.773$, $P \leq 0.030$). Significantly lower JA levels than in AZ wild type were detected in small buds (Fig. 3D, left section; Bonferroni-corrected post-hoc test ANOVA, $F_{2,12} = 8.465$, $P \leq 0.0334$) and in flowers (Fig. 3F, left section; ANOVA, Bonferroni-corrected post-hoc test, $F_{2,11} = 9.758$, $P \leq 0.0051$) but not in medium-sized buds (Fig. 3E, left section; ANOVA, Bonferroni-corrected post-hoc test, $F_{2,14} = 1.014$, $P > 0.05$) of AZ transgenic lines. Interestingly, the accumulation of ppHS transcripts during flower development did not vary significantly (Supplemental Fig. S5).

Levels of Abscisic Acid, Auxins, and Ethylene in *NappHS*-Silenced Buds and/or Flowers

Since flower development is under the regulation of many interacting hormones such as abscisic acid (ABA), auxins, and ethylene, we measured these hormones as well. ABA's role in flower senescence is known, and that ABA treatment increased ppHS transcripts in cultivated tobacco has been described (Rocha-Granados et al., 2005). We found no significant difference in the ABA contents among the AZ (Supplemental Fig. S6, A–C, left section; ANOVA, Bonferroni-corrected post-hoc test, $P > 0.05$) or UT lines (Supplemental Fig. S6, A–C, left section; ANOVA, Bonferroni-corrected post-hoc test, $P > 0.05$), or their respective silenced lines. Levels of indole-3-acetic acid (IAA), the most impor-

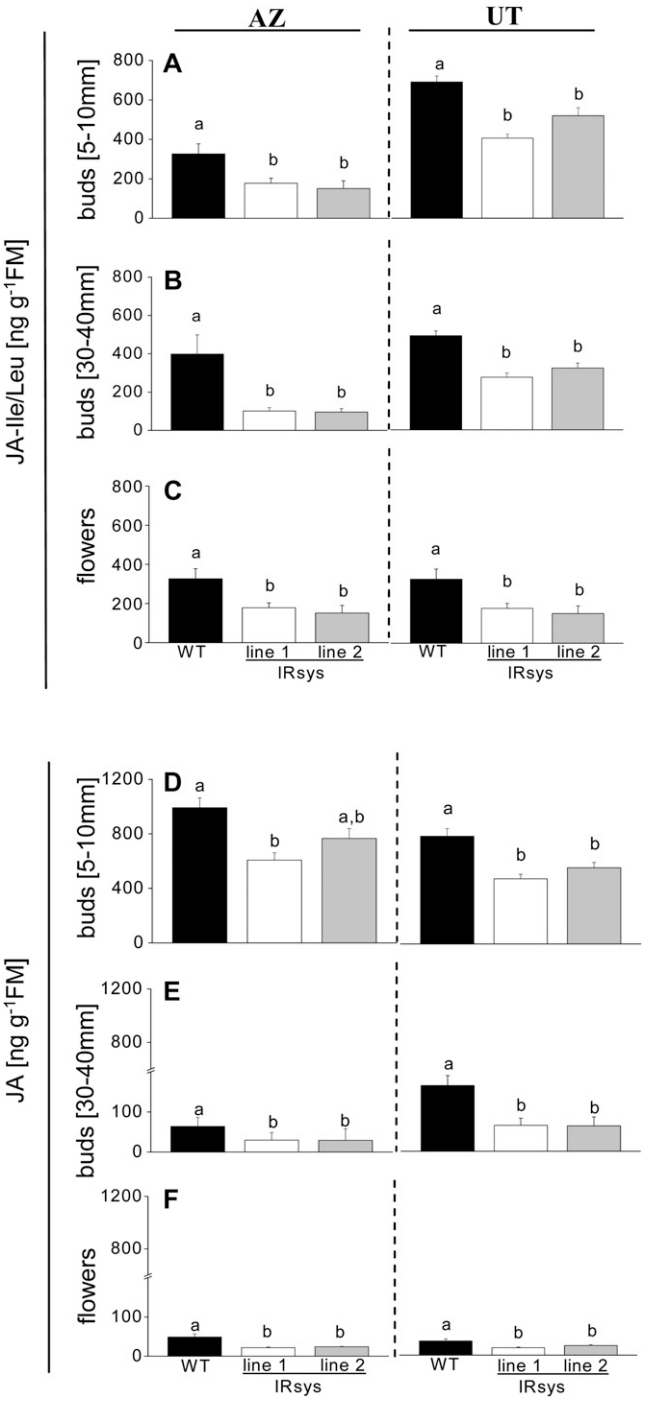

Figure 3. *NappHS*-silenced buds and flowers accumulate lower levels of JAs. Mean ± SE JA-Ile/Leu and JA contents of four to five small (A and D, 5–10 mm) and elongated (B and E, 30–40 mm) buds and flowers (C and F) of wild type (WT; black bars), IRsys line 1 (white bars), and IRsys line 2 (gray bars) of AZ (left section) and UT (right section) accessions. Different letters indicate significant differences (ANOVA followed by Bonferroni-corrected post-hoc test).

tant auxin in plants, did not differ in buds among the genotypes. Only IRsys line 2 of the AZ accession showed reduced IAA levels (Supplemental Fig. S7). Ethylene is known to be emitted from flowers in response to pollination (for review, see O'Neill, 1997) and can be a sensitive indicator of differences in auxin signaling. As expected from the pollination-limited seed set of IRsys flowers (Fig. 1), ethylene emissions were lower from self-pollinated IRsys flowers than from wild-type flowers of both accession (Supplemental Fig. S8, AZ: IRsys line 1 and UT: IRsys line 1; ANOVA, Bonferroni-corrected post-hoc test, $P < 0.05$). Hand-pollinated flowers of the same genotypes did not differ in ethylene emissions in comparison to their respective wild types (Supplemental Fig. S8), demonstrating that differences in pollination, rather than ethylene signaling, were responsible for the lower ethylene emissions of IRsys flowers.

Transcriptional Profiling of JA Biosynthesis Genes

To understand how silencing *ppHS* influences JA accumulation in flowers, we isolated RNA from stamens, pistil, and corolla and measured relative transcript abundances of *NaAOS*, *NaLOX3*, *NaJAR4*, *NaJAR6*, and *NaTD* using real-time qPCR. *NaAOS*, the gene that encodes the allene oxidase synthase, and *NaLOX3*, the gene that encodes a lipoxygenase, are known to directly influence JA accumulation. The relative transcript abundance of both genes was not lower in stamens, pistils, and corollas of IRsys flowers compared to wild-type flowers (Supplemental Fig. S9A, *NaLOX3*; ANOVA, Bonferroni-corrected post-hoc test, $P > 0.05$; and *NaAOS*; ANOVA, Bonferroni-corrected post-hoc test, $P > 0.05$), indicating that the absence of ppHS in *N. attenuata* flowers does not impair the transcriptional regulation of enzymes involved in JA production. Since we found significantly lower levels of JA-Ile/Leu in buds and flowers of IRsys plants in AZ and UT, we measured transcript levels of *NaTD* and *NaJAR4*/*NaJAR6*. Thr deaminase (TD) is involved in the synthesis of Ile, and *NaJAR4*/*NaJAR6* genes encode enzymes responsible for conjugating JA and Ile (Kang et al., 2006; Wang et al., 2007). We did not detect significant differences in *NaJAR4* transcripts between AZ IRsys and the AZ wild-type flower parts (Supplemental Fig. S9C, left section; ANOVA, Bonferroni-corrected post-hoc test, $P > 0.05$), or between UT IRsys and UT wild-type flower parts (Supplemental Fig. S9C, right section; ANOVA, Bonferroni-corrected post-hoc test, $P > 0.05$). Similar results were obtained from real-time qPCR analysis of the second gene known to be responsible for the conjugation step, *NaJAR6* (Supplemental Fig. S9D; ANOVA, $P > 0.05$). These data suggest that ppHS-silenced flowers do not differ from wild-type flowers in JA biosynthesis and JA conjugation activity. However, differences in TD transcript levels were found. While *NaTD* levels in corolla and stamen tissues and the TD activity in buds (Supplemental Fig. S10) did not differ among the genotypes, the pistils of IRsys-silenced flowers had significantly lower levels of *NaTD* transcripts in both accessions (AZ, Fig. 4, left section; ANOVA, $P < 0.0315$; UT, Fig. 4, right section; ANOVA, Bonferroni-corrected post-hoc test, $P \leq 0.0078$).

DISCUSSION

Both systemins and HypSys belong to a functionally defined gene family whose members are supposed to amplify defense signaling pathways. Known functional similarities between systemin and HypSys peptides or their precursors are not reflected in their phylogenetic relationships (Supplemental Fig. S11). Interestingly, the phylogenetically more similar HypSys peptides appear to be more functionally diverse than the more distantly related tomato systemin and the cultivated tobacco HypSys, as evidenced by studies in tomato, cultivated tobacco, and petunia. Recently, HypSys peptides in tomato and cultivated tobacco were found to activate defense genes in response to wounding and herbivore attack (Pearce et al., 2001; Rocha-Granados et al., 2005), and transgenic cultivated tobacco plants ectopically expressing the HypSys precursor were found to be less susceptible to *Helicoverpa armigera* larvae (Ren and Lu, 2006). Although HypSys peptides isolated from petunia did not induce defense genes directed against herbivores, they did activate

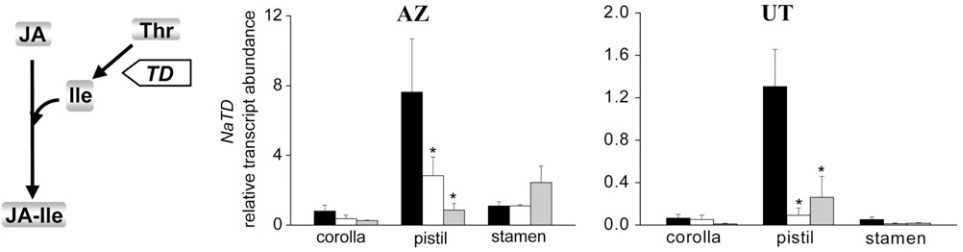

Figure 4. Silencing *NappHS* reduces TD transcript abundance in corolla, pistil, and stamens from wild-type (black bars), IRsys line 1 (white bars), and IRsys line 2 (gray bars) flowers of AZ (middle section) and UT (right section) accessions. TD expression is required for the production of JA-Ile. TD catalyzes the formation of α-keto butyrate from Thr, the first step in biosynthesis of Ile, which is conjugated to JA (left section).

defensin1, a gene involved in pathogen defense (Pearce et al., 2007). Surprisingly, we found that the cultivated tobacco prosystemin precursor homolog did not play a central role in *N. attenuata*'s (accession Utah) antiherbivore defense signaling, such as in TPI or nicotine production (Berger and Baldwin, 2007).

Due to the apparent rapid diversification of function among HypSys homologs, we hypothesized that *NappHS* may have lost its defensive function in UT recently and extended our analysis to include a different accession, AZ, which unlike UT is unable to produce TPIs. Because TPIs are not present in AZ and because nicotine is a representative JA-induced defense compound that is present in both AZ and UT (Glawe et al., 2003), we asked if nicotine production is affected by *NappHS* expression. Given that nicotine was elicited independently of *NappHS* expression in both AZ (Supplemental Fig. S1D) and UT accessions, we conclude that *NappHS* is not directly involved in the antiherbivore defense of either accession.

If *NappHS* is not involved in the defense responses of *N. attenuata*, why are *NappHS* transcripts expressed in aboveground tissue, and why are they particularly abundant in flowers (Berger and Baldwin, 2007)? It is known that Hyp-rich glycoproteins are widely distributed in plants, and their expression is frequently tissue specific and temporally regulated. Some are expressed in young leaves (soybean [*Glycine max*]; Hong et al., 1987) and in reproductive tissues (*Nicotiana alata* and cultivated tobacco; Sommer-Knudsen et al., 1998), which suggested that *NappHS* might function in reproduction. The hypothesis was corroborated by the fact that self-pollinating IRsys plants growing in the glasshouse produced fewer seed capsules and their capsules contained fewer seeds per capsule compared to wild-type plants (Fig. 1A). Silencing the HypSys precursor in cultivated tobacco would be an interesting follow-up experiment to determine if HypSys of both *Nicotiana* species shared similar nondefensive functions. Moreover, such an experiment would clarify whether the silencing of HypSys precursors results in fitness costs unrelated to herbivore-induced defense metabolite production in cultivated tobacco.

How *NappHS* contributes to seed capsule production in *N. attenuata* needs to be clarified. Our growth data excluded differences in vegetative biomass as a possible reason for the observed differences in seed capsule production (Supplemental Fig. S2, A and B). Dysfunctions in fertility could be ruled out as hand-pollination experiments revealed that neither reduced pollen nor ovule viability could account for the reduced reproductive performance of IRsys plants (Supplemental Fig. S3; Fig. 1B). Since hand-pollination restored the numbers of seeds produced in IRsys plants to those of wild-type plants, we inferred that silencing *NappHS* reduces the self-pollination frequency under glasshouse conditions and consequently reduces seed yield. It seems likely that reduced self-pollination rates are the reason for the observed yield losses rather than an inhibition in the maturation of male and female flower organs, as seen in other flower mutants impaired in fruit and seed production. For example, the *jasmonic acid-insensitive-1* (*jai-1*) tomato mutant showed no growth phenotype, but was impaired in fruit and seed production similar to IRsys plants. Reciprocal crossing experiments with wild-type tomato and *jai-1* plants clearly revealed that the sterility of this mutant was based on dysfunctions in the female reproductive organs (Li et al., 2001).

N. attenuata flowers characteristically contain a pistil surrounded by five stamens: a long pair of stamens at the mouth of the corolla, a shorter pair of stamens, and a single stamen shorter than the others (Goodspeed et al., 1954). During elongation of the corolla but before corolla opens, the stigma passes through the dehisced anthers, and the fertilization process is initiated. If the anthers do not dehisce or if dehiscence is delayed, self-pollination is reduced. In the case of IRsys flowers, the stigma has already passed the anthers before the anthers dehisce and open flowers have a highly visible stigma that protrudes beyond the anthers (Fig. 2A; Supplemental Fig. S12). The greater distance between the male and the female parts of IRsys flowers was due to a longer pistil (Fig. 2B), the part of the flower with the highest *NappHS* transcript levels (Fig. 2D). Since IRsys stamens were not shorter than wild-type stamens, we propose that this distance is the result of morphological changes in the pistil.

Changes in flower morphology are commonly described in plants impaired or mutated in JA signaling (Sanders et al., 2000; Stintzi and Browse, 2000; Ishiguro et al., 2001; Park et al., 2002; Mandaokar et al., 2003), and examples of plants with modified JA contents are also known from *N. attenuata*. *N. attenuata* plants silenced in *COI1* are insensitive to JA and plants silenced in *TD* are impaired in JA-Ile production. These two genotypes also exhibit abnormal flower phenotypes (Kang, 2006; Paschold et al., 2007) that resemble those of *NappHS*-silenced plants. JA and JA-Ile/Leu measurements revealed that the phenotypic changes of IRsys flowers are correlated with decreased levels of JA-Ile/Leu in flowers (Fig. 3C). In contrast to the reduced JA levels in flowers, we found no differences in JA content in IRsys leaves and also not 1 h after wounding and elicitation with oral secretions of *M. sexta* larvae (Berger and Baldwin, 2007). Therefore we suppose a tissue- and time-specific function for HypSys peptides in *N. attenuata*. Whether the strong *NappHS* transcript abundance in flowers might also reflect an involvement of *NappHS* in antipathogen defense to protect the reproductive organs is another interesting aspect that could be tested since HypSys peptides in petunia are involved in antipathogen defense.

Interestingly, JA levels decrease precipitously during flower development in both AZ and UT accessions, while JA-Ile levels decrease only modestly (Fig. 3), suggesting that JA-Ile/Leu or other JA conjugates play a more important role in *N. attenuata* flower development than JA itself. Similar findings in tomato cv Moneymaker buds and flowers, which contain more

JA-Ile than JA (Hause et al., 2000), are consistent with this view.

Changes in the JA profiles of IRsys flowers are mirrored in the abundance of transcripts of JA, JA-Ile/Leu biosynthetic genes, and TD. TD catalyzes the formation of α-ketobutyrate (α-KB) from Thr, the first step in the biosynthesis of Ile that is conjugated to JA. Transcripts of JA biosynthesis and JA-Ile/Leu conjugation enzyme genes did not differ from those in wild-type flowers (Supplemental Fig. S9), but *TD* expression was reduced in the female parts of IRsys flowers (Fig. 4), suggesting that ppHS influences JA signaling by regulating TD expression. *N. attenuata* plants with reduced endogenous TD levels reveal several morphological changes including shortened pistils and petaloid anthers. Low levels of TD are correlated with low levels of JA-Ile/Leu in floral buds (Kang, 2006), a pattern that was also seen in IRsys buds (Fig. 3A). While IRsys buds contain less JA than wild-type buds do, silencing TD was associated with a 1.3-fold increase of JA in buds (Kang, 2006). We propose that the tissue-specific down-regulation of TD transcripts in pistils of IRsys flowers results in imbalances in the relative proportion of JAs in this floral organ. These imbalances might lead to the elongated pistils in IRsys flowers. The delicate balancing of time- and tissue-specific JA profiles is important during flower development as demonstrated by Hause et al. (2000). Developmental phenotypes are notoriously difficult to complement or recover, which could explain why our attempts to restore the wild-type phenotype in IRsys flowers by stem-feeding flowering stems with 0.1 mM JA, JA-Ile, or indanone (a JA-Ile mimic), or by dipping inflorescences in a 0.05 mM methyl-JA solutions two times a day for 3 d were not successful.

Another hypothesis why JA complementation failed to restore the wild-type phenotype is that JAs only influence a particular aspect of the IRsys flower phenotype and that other, not-yet-identified factors play a role as well. Another phytohormone could be one of these factors. Hormones known to play central roles in flower development are ethylene (e.g. Vanaltvorst and Bovy, 1995; Rieu et al., 2003) and auxins (e.g. Naderi et al., 1997; Oka et al., 1998; Al-Hammadi et al., 2003). Auxins regulate the development of both stamens and pistils (Cecchetti et al., 2004). In Arabidopsis (*Arabidopsis thaliana*), two paralogous auxin response transcription factors, ARF6 and ARF8, are known to regulate stamen and gynoecium maturation, and an *arf6 arf8* double-null mutant produces flowers with undehisced anthers and immature gynoecia. *Arf6 arf8* double-null mutants contain JA concentrations below the detection limit but endogenous application of JA could restore only anther dehiscence but not gynoecia maturation (Nagpal et al., 2005). Relative IAA levels were reduced only in buds of one IRsys line (Supplemental Fig. S6), contrasting to the clear reduction of JAs in all investigated IRsys buds and flowers (Fig. 3). Moreover hand-pollination experiments with IRsys flowers could restore the seed set to wild-type levels. This suggests that anther and gynoecia maturation was not affected in IRsys flowers and hormone signaling, such as the polar auxin transport that is involved in pollination and fertilization processes was not impaired in IRsys flowers. Auxin and ethylene signaling are known to be associated with pollination and fertilization. Pollination results in ethylene production in many flowers, which triggers senescence of the corolla and fruit ripening (O'Neill, 1997); this pollination-induced ethylene response did not differ between hand-pollinated wild-type and IRsys flowers (Supplemental Fig. S7B).

The role of ethylene in pistil growth regulation was recently highlighted by Hibi et al. (2007). The TEIL (for Tobacco EIN3-Like) gene is a tobacco homolog of Arabidopsis Ethylene Insensitive3 (EIN3), a protein encoding a key transcriptional factor in ethylene signaling. Overexpression of both genes in the respective species was associated with protruded pistils (Guo and Ecker, 2003; Hibi et al., 2007) similar to the flower phenotype found in *NappHS*-silenced *N. attenuata* plants. Interestingly, flowers silenced in TEIL also exhibit pistil protrusion, demonstrating that the underlying mechanisms may be complex and related to differential perception of ethylene rather than increased or reduced sensitivity to this hormone. Whether ethylene contributes to the protruded pistil in IRsys flowers of *N. attenuata* is not clear yet, because reduced ethylene emissions in self-pollinated IRsys flowers could be simply the result of low pollination rates (Supplemental Fig. S7A).

However the phenotype cannot be fully explained by a decrease only in JAs, even though it seems that they play a central role in interacting with ppHS, and more research is required to understand how *NappHS* regulates pistil length.

The question remains as to why IRsys flowers possess longer pistils. Changes in style length in cultivated tomato flowers were recently attributed to a mutation of the promoter of *Style2.1*, a gene that encodes a putative transcription factor regulating cell elongation in developing styles. *Style2.1* was identified by quantitative trait loci mapping as a major factor for flower development and the changes in style length lead to a switch from cross-pollination to self-pollination (Chen et al., 2007). Silencing *NappHS* results in longer pistils and the ability to switch from self-pollination to outcrossing. Outcrossing increases genetic diversity and perhaps increases fitness in plants such as *N. attenuata* that are adapted to germinate and grow in exceptionally unpredictable environments.

MATERIALS AND METHODS

Plant Material and Growing Conditions

Nicotiana attenuata Torr. Ex. Wats. seeds from a Utah population originally collected near Santa Clara, Utah, and inbred for 14 or 15 generations were used to conduct experiments and to generate transformed lines from this accession (UT). Seeds of the Arizona accession (AZ) were collected from a 20-

plant population near Flagstaff, Arizona (Glawe et al., 2003), and the seventh generation inbred line was used in all experiments and to generate the transformed lines. For glasshouse experiments, seeds were germinated as described by Krügel et al. (2002). Plants were grown in 1-L pots at 26°C to 28°C under 16 h of light supplemented by Philips Sun-T Agro 400- and 600-W Na lights.

Generation of IRsys Lines

Cloning and sequencing the NapreproHypSys gene (*NappHS*; GenBank accession no. AY456270) and the generation of IRsys lines for the Utah accession (line 1: A-04-366-11; line 2: A-04-464-1) are described by Berger and Baldwin (2007). IRsys lines of the Arizona accession (line 1: A-04-357-11; line 2: A-04-385-13) were generated with the same vector (pRESC5sys2), and they were tested for their ploidy level as described by Bubner et al. (2006).

Nucleic Acid Analysis

To determine the number of transformation vector insertions in the transformed lines of the AZ accession, isolated genomic DNA was hybridized with a PCR fragment of the *hptII* gene, the selection marker used on the transformation vector (pRESC). The PCR product for both probes was eluted from the gel using a Geneclean kit (BIO 101; Vista), labeled with $^{[32]}$P using a random prime labeling kit (RediPrime II; Amersham-Pharmacia), and purified on G50 columns (Amersham-Pharmacia). After overnight hybridization, blots were washed one time with 2× sodium chloride/sodium phosphate/EDTA at 62°C and three times with 2× chloride/sodium phosphate/EDTA/2% SDS, and analyzed with a phosphor-imager (model FLA-3000; Fuji Photo Film Co.).

To quantify transcripts in leaves and flower tissue (stamens, corolla, and pistil) and at different developmental flower stages, total RNA was extracted using TRI Reagent (Sigma) according to the protocol of Chomczynski and Sacchi (1987), with minor modifications for polysaccharide-rich plant tissue to minimize the coprecipitation of impurities. An additional salt buffer (1.2 M $NaCl_2$, 0.8 M sodium citrate) was added to the isopropanol precipitation step.

For real-time quantification of the transcripts, cDNA was prepared from 200 ng total RNA with MultiScribe reverse transcriptase (Applied Biosystems). The gene-specific primers and probes for *NappHS*, *NaLOX3*, *NaAOS*, *NaJAR4*, *NaJAR6*, and *NaTD* mRNA expression detection by qPCR are provided in Supplemental Table S1. The assays using a double-dye-labeled probe were performed on an ABI PRISM 7700 Sequence Detection system (qPCR Core kit; Eurogentec). The expression of each gene was normalized to the expression of the endogenous control gene actin. Northern-blot analysis of ppHS transcripts in AZ wild-type plants was conducted as described by Berger and Baldwin (2007).

Growth, Fitness Performance, and Flower Morphology Analysis

Stalk length measurements in elongating 4-week-old plants were made over a period of 2 weeks to evaluate growth. First flowering, flower number, and lifetime seed capsule numbers were determined as estimates of fitness. Freshly opened flowers were counted in 40-d-old plants and total seed capsule number was counted after irrigation was stopped. Aboveground tissue was collected and dried at 60°C, and biomass was determined.

To determine the seeds per capsule of self-pollinated plants, the first four to five ripe seed capsules of each genotype were collected and dried, and seeds were counted. In an additional setup, flowers with nondehisced anthers of each genotype were emasculated with forceps, and 1 d later the opened flowers were pollinated by hand with pollen of the same genotype. After seed capsules had ripened, the number of seeds per capsule was counted.

Pollen grains from each genotype were stained with fluoresceine diacetate to determine their viability. A fluorescine diacetate stock (60 mg dissolved in 30 mL acetone) was added to a 10% (w/v) Suc solution until it turned milky. A drop of this solution was placed onto a glass slide, and dehisced anthers were dipped into this solution before being incubated for 5 min. Viable pollen was visualized under a fluorescence microscope.

Fully opened flowers from each genotype were dissected with a scalpel, and the distances between the anther of the longest filament and the stigma, as well as the total length of each stamen and the pistil, were measured with a caliper.

Phytohormone Analysis

Approximately 150 mg tissue from five small buds (5–10 mm), green buds (30–40 mm), or fully opened flowers of each accession and genotype were harvested. The flash-frozen tissue was homogenized and extracted in FastPrep tubes containing 0.9 g of FastPrep Matrix (BIO 101), and 1 mL ethyl acetate containing methanolic 200 ng mL^{-1} [$^{13}C_2$]JA and 200 ng mL^{-1} [D_6]ABA was added as the internal standards. JA-Ile concentrations were calculated based on an external standard dilution series of JA-Ile. The FastPrep tubes were shaken two times at 6.0 m s^{-1} for 45 s. Samples were centrifuged at 13,000 rpm for 20 min at 4°C and the supernatant was collected. The extraction step was repeated with 1 mL ethyl acetate. Both supernatants were combined and evaporated in a SpeedVac concentrator. The dried samples were dissolved in 500 μL MeOH (70%) and centrifuged for 10 min at 13,000 rpm at 4°C. Analysis of the samples was performed using a Varian 1200L Triple-Quadrupole-LC-MS (Varian) as described by Wang et al. (2007).

To measure IAA, approximately 100 to 200 mg of frozen bud tissue was ground in liquid nitrogen, 500 μL of 1-propanol/water/concentrated HCL (2:1:0.002, vol/vol/vol) with IAA-D_5 as the internal standard. The samples were agitated at a Thermomixer (Eppendorf), for 30 min at 4°C, 1 mL CH_2CL_2 was added followed by an agitation for 30 min. Samples were centrifuged at 13,000 rpm for 5 min, the lower layer was concentrated in a vacuum concentrator (Eppendorf), and resolubilized in 100 μL MeOH. Hormone extracts (10 μL aliquot) were analyzed by reverse-phase HPLC coupled to tandem mass spectrometry as described by Wu et al. (2007). Multiple reactions monitoring was conducted with a 1200L MS/MS/MS system (Varian), after negative ionization, with parent-26 ion/daughter-ion selections: 174/130 (IAA), 179/135 (IAA-D_5). The area beneath the multiple reactions monitoring product ion peak was determined for each analyte and internal standard (IS). The quantity of the analyte was calculated according to the formula: analyte product ion peak area × (IS concentration/IS product ion peak area).

Ethylene emissions were measured in hand-pollinated and self-pollinated flowers. Buds with unopened anthers were emasculated the evening before the measurement, labeled, and hand-pollinated the next morning. Hand-pollinated flowers were immediately transferred to 100 mL cuvettes, and ethylene was allowed to accumulate in the headspace for 5 h or as otherwise indicated. For the ethylene measurement of self-pollinated flowers all open flowers were removed from the plant, and buds of the same developmental stage as those used for hand-pollination were labeled the evening before. Opened flowers were transferred to the cuvettes the next morning. Stop-flow measurements were taken continuously and noninvasively in real time with a photoacoustic spectrometer (INVIVO) as described by von Dahl et al. (2007).

Nicotine

After AZ and AZ IRsys leaves of the same position (defined as +2) were wounded with a pattern wheel, 20 μL deionized water was applied three times in a row, every 30 min. The nicotine content in unwounded control plants and in wounded AZ and AZ IRsys plants was determined as described by Keinänen et al. (2001) with the modification that approximately 100 mg frozen tissue was homogenized in 1 mL extraction buffer utilizing the FastPrep extractions system (Savant Instruments).

TD Activity

Flash-frozen flowers and buds (approximately 200 mg) were homogenized in 2 volumes of extraction buffer (100 mM Tris buffer, pH 9, 100 mM KCl, and 10 mM β-mercaptoethanol) and centrifuged at 15,000*g* for 15 min at 48°C. TD activity was assayed by incubating the enzyme with substrate and determining the quantity of α-KB formed. The α-KB was estimated by modifying the method described by Sharma and Mazumder (1970). Protein extract (100 mL) was added to the same volume of reaction buffer (40 mM L-Thr, 100 mM Tris buffer, pH 9, and 100 mM KCl). After incubation at 37°C for 30 min, 160 mL of 7.5% trichloracetic acid was added to stop the reaction, and the protein precipitate was removed by centrifugation at 10,000*g* for 2 min. α-KB was determined by adding 400 mL of 0.05% dinitrophenylhydrazine in 1 N HCL to the sample solution. After incubation at room temperature for 10 min, 400 mL of 4 N sodium hydroxide was added to the sample solution and mixed well. After incubation at room temperature for 20 min, the absorbance of the sample solution was read at 505 nm in a spectrophotometer (model Ultraspec 3000; Pharmacia Biotech).

Phylogenetic Analysis of ProHypSys/HypSys and ProSys/Sys Protein Sequences

A Bayesian phylogenetic analysis of ProSys and ProHypSys, as well as of the deduced Sys and HypSys sequences from *Capsicum annuum* (*Ca* ProSys: AF000375), *Nicotiana attenuata* (NaProHypSys: AY456270), *Nicotiana tabacum* (NtProHypSys-A: AY033148, NtProHypSys-B: AY033149), *Petunia hybrida* (PhProHypSys: EF552428), *Solanum lycopersicum* (SlProHypSys: AY292201; SlProSys: M84801), *Solanum nigrum* (SnProSys: AF000375), and *Solanum tuberosum* (StProSys_1: AF000373, StProSys_2: AF000374) was conducted. Amino acid sequences were aligned with ClustalW. Target peptides and alignment gaps were excluded. The tree was constructed with MrBayes v 3.1.2 (Huelsenbeck and Ronquist, 2001) using a mixed amino acid substitution model approach. Data structure was best explained by the Jones model (Whelan and Goldman, 2001) with a posterior probability of 1.000. The Markov-Chain-Monte-Carlo simulation was performed in three parallel runs with four chains each for 1,000,000 iterations with a sample frequency of 200 and a burnin fraction of 0.05. Convergence diagnostic over all three runs (potential scale reduction factor) was 1.000. Shown are posterior probabilities for all internal nodes.

Statistical Analysis

Data were analyzed with Statview 5.0 (SAS Institute). Data were transformed if they did not meet the assumption of homoschedacity.

Supplemental Data

The following materials are available in the online version of this article.

Supplemental Figure S1. Northern-blot analysis of *NappHS* transcripts in AZ wild-type plants.

Supplemental Figure S2. *NappHS*-silenced plants do not differ from wild-type plants in flower production or stalk elongation.

Supplemental Figure S3. Viability of pollen from wild-type and IRsys flowers.

Supplemental Figure S4. Percentage of flowers with elongated pistils.

Supplemental Figure S5. Mean ± SE ABA content of four to five small (A, 5–10 mm) and elongated (B, 30–40 mm) buds and flowers of wild type (black bars) and IRsys line 1 (white bars) and IRsys line 2 (gray bars) AZ (left section) and UT (right section) accessions.

Supplemental Figure S6. IAA concentration in wild-type and IRsys buds.

Supplemental Figure S7. Ethylene emissions are reduced in self-pollinated but not in hand-pollinated IRsys flowers.

Supplemental Figure S8. Relative transcript abundance of *NappHS* in small buds (s-bud), buds (l-bud), and flowers (flo) of AZ (gray bars) and UT (black bars) wild-type plants.

Supplemental Figure S9. Transcript accumulation of genes involved in JA synthesis and in the conjungation step of JA with Ile in the oxylipin pathway.

Supplemental Figure S10. α-KB concentration in buds of four to five replicates from AZ and UT wild type (black bars) and their respective inverted repeat (IRsys) lines 1 (white bars) and lines 2 (gray bars).

Supplemental Figure S11. Phylogenetic relationship of NaHypSys and HypSys as well as Sys from other plant species (A) and of NaProHypSys, ProHypSys, and ProSys of other plant species (B; based on deduced amino acid sequences).

Supplemental Figure S12. AZ wild-type and IRsys flowers at different developmental stages.

Supplemental Table S1. Gene-specific primers and probes used for real-time qPCR.

ACKNOWLEDGMENTS

We thank Dr. Klaus Gase for generating the transformation vector, Susan Kutschbach and Antje Wissgott for transforming the plants, Dr. Tamara Krügel for guidance in the flower pollination experiment, Markus Benderoth for invaluable help on the phylogenetic analysis, Eva Rothe and Dr. Matthias Schöttner for technical assistance in phytohormone analysis, and Emily Wheeler for editorial assistance.

Received December 22, 2008; accepted January 29, 2009; published February 11, 2009.

LITERATURE CITED

Al-Hammadi ASA, Sreelakshmi Y, Negi S, Siddiqi I, Sharma R (2003) The polycotyledon mutant of tomato shows enhanced polar auxin transport. Plant Physiol **133:** 113–125

Baldwin IT (2001) An ecologically motivated analysis of plant-herbivore interactions in 20 native tobacco. Plant Physiol **127:** 1449–1458

Berger B, Baldwin IT (2007) The hydroxyproline-rich glycopeptide systemin precursor *Na*preproHypSys does not play a central role in *Nicotiana attenuata*'s anti-herbivore defense responses. Plant Cell Environ **30:** 1450–1464

Bubner B, Gase K, Berger B, Link D, Baldwin IT (2006) Occurrence of tetraploidy in *Nicotiana attenuata* plants after *Agrobacterium*-mediated transformation is genotype specific but independent of polysomaty of explant tissue. Plant Cell Rep **25:** 668–675

Cecchetti V, Pomponi M, Altamura MM, Pezzotti M, Marsilio S, D'Angeli S, Tornielli GB, Costantino P, Cardarelli M (2004) Expression of rolB in tobacco flowers affects the coordinated processes of anther dehiscence and style elongation. Plant J **38:** 512–525

Chen KY, Cong B, Wing R, Vrebalov J, Tanksley SD (2007) Changes in regulation of a transcription factor lead to autogamy in cultivated tomatoes. Science **318:** 643–645

Chomczynski P, Sacchi N (1987) Single-step method of RNA isolation by acid guanidinium thiocyanate phenol chloroform extraction. Anal Biochem **162:** 156–159

Glawe G, Zavala JA, Kessler A, van Dam NM, Baldwin IT (2003) Ecological costs and benefits correlated with trypsin protease inhibitor production in *Nicotiana attenuata.* Ecology **84:** 79–90

Goodspeed TH, Wheeler HM Hutchinson (1954) Taxonomy of *Nicotiana*. *In* TH Harper, ed, The Genus *Nicotiana*, Vol 16. Chronica Botanica, Waltham, MA, pp 427–430

Guo HW, Ecker JR (2003) Plant responses to ethylene gas are mediated by SCF (EBF1/EBF2)-dependent proteolysis of EIN3 transcription factor. Cell **115:** 667–677

Hause B, Stenzel I, Miersch O, Maucher H, Kramell R, Ziegler J, Wasternack C (2000) Tissue-specific oxylipin signature of tomato flowers: allene oxide cyclase is highly expressed in distinct flower organs and vascular bundles. Plant J **24:** 113–126

Hibi T, Kosugi S, Iwai T, Kawata M, Seo S, Mitsuhara I, Ohashi Y (2007) Involvement of EIN3 homologues in basic PR gene expression and flower development in tobacco plants. J Exp Bot **58:** 3671–3678

Hong JC, Nagao RT, Key JL (1987) Characterization and sequence-analysis of a developmentally regulated putative cell-wall protein gene isolated from soybean. J Biol Chem **262:** 8367–8376

Huelsenbeck JP, Ronquist F (2001) MRBAYES: Bayesian inference of phylogenetic trees. Bioinformatics **17:** 754–755

Ishiguro S, Kawai-Oda A, Ueda J, Nishida I, Okada K (2001) The DEFECTIVE IN ANTHER DEHISCENCE1 gene encodes a novel phospholipase A1 catalyzing the initial step of jasmonic acid biosynthesis, which synchronizes pollen maturation, anther dehiscence, and flower opening in *Arabidopsis*. Plant Cell **13:** 2191–2209

Kang JH (2006) The roles of threonine deaminase in *Nicotiana attenuata*. PhD thesis. Friedrich-Schiller-Universität, Jena, Germany

Kang JH, Wang L, Giri A, Baldwin IT (2006) Silencing threonine deaminase and *JAR4* in *Nicotiana attenuata* impairs jasmonic acid-isoleucine-mediated defenses against *Manduca sexta.* Plant Cell **18:** 3303–3320

Keinänen M, Oldham NJ, Baldwin IT (2001) Rapid HPLC screening of jasmonate-induced increases in tobacco alkaloids, phenolics, and diterpene glycosides in *Nicotiana attenuata.* J Agric Food Chem **49:** 3553–3558

Krügel T, Lim M, Gase K, Halitschke R, Baldwin IT (2002) *Agrobacterium*-mediated transformation of *Nicotiana attenuata*, a model ecological expression system. Chemoecology **12:** 177–183

Li L, Li CY, Howe GA (2001) Genetic analysis of wound signaling in

tomato: evidence for a dual role of jasmonic acid in defense and female fertility. Plant Physiol **127:** 1414–1417

Mandaokar A, Kumar VD, Amway M, Browse J (2003) Microarray and differential display identify genes involved in jasmonate-dependent anther development. Plant Mol Biol **52:** 775–786

McGurl B, Pearce G, Orozco-Cárdenas M, Ryan CA (1992) Structure, expression, and antisense inhibition of the systemin precursor gene. Science **255:** 1570–1573

Naderi M, Caplan A, Berger PH (1997) Phenotypic characterization of a tobacco mutant impaired in auxin polar transport. Plant Cell Rep **17:** 32–38

Nagpal P, Ellis C, Weber H, Ploense S, Barkawi L, Guilfoyle T, Hagen G, Alonso J, Cohen J, Farmer E, et al (2005) Auxin response factors ARF6 and ARF8 promote jasmonic acid production and flower maturation. Development **132:** 4107–4118

Narváez-Vásquez J, Orozco-Cárdenas M, Ryan C (2007) Systemic wound signaling in tomato leaves is cooperatively regulated by systemin and hydroxyproline-rich glycopeptide signals. Plant Mol Biol **65:** 711–718

Oka M, Ueda J, Miyamoto K, Okada K (1998) Activities of auxin polar transport in inflorescence axes of flower mutants of *Arabidopsis thaliana*: relevance to flower formation and growth. J Plant Res **111:** 407–410

O'Neill SD (1997) Pollination regulation of flower development. Annu Rev Plant Physiol Plant Mol Biol **48:** 547–574

Park JH, Halitschke R, Kim HB, Baldwin IT, Feldmann KA, Feyereisen R (2002) A knock-out mutation in allene oxide synthase results in male sterility and defective wound signal transduction in *Arabidopsis* due to a block in jasmonic acid biosynthesis. Plant J **31:** 1–12

Paschold A, Halitschke R, Baldwin IT (2007) Co(i)-ordinating defenses: *Na*COI1 mediates herbivore-induced resistance in *Nicotiana attenuata* and reveals the role of herbivore movement in avoiding defenses. Plant J **51:** 79–91

Pearce G, Moura DS, Stratmann J, Ryan CA (2001) Production of multiple plant hormones from a single polyprotein precursor. Nature **411:** 817–820

Pearce G, Ryan CA (2003) Systemic signaling in tomato plants for defense against herbivores—isolation and characterization of three novel defense-signaling glycopeptide hormones coded in a single precursor gene. J Biol Chem **278:** 30044–30050

Pearce G, Siems WF, Bhattacharya R, Chen YC, Ryan CA (2007) Three hydroxyproline-rich glycopeptides derived from a single petunia polyprotein precursor activate defensin I, a pathogen defense response gene. J Biol Chem **282:** 17777–17784

Ren F, Lu YT (2006) Overexpression of tobacco hydroxyproline-rich glycopeptide systemin precursor A gene in transgenic tobacco enhances resistance against *Helicoverpa armigera* larvae. Plant Sci **171:** 286–292

Rieu I, Wolters-Arts M, Derksen J, Mariani C, Weterings K (2003) Ethylene regulates the timing of anther dehiscence in tobacco. Planta **217:** 131–137

Rocha-Granados MC, Sánchez-Hernández C, Sánchez-Hernández CV, Martínez-Gallardo NA, Ochoa-Alejo N, Délano-Frier JP (2005) The expression of the hydroxyproline-rich glycopeptide systemin precursor A in response to (a)biotic stress and elicitors is indicative of its role in the regulation of the wound response in tobacco (*Nicotiana tabacum* L.). Planta **222:** 794–810

Sanders PM, Lee PY, Biesgen C, Boone JD, Beals TP, Weiler EW, Goldberg RB (2000) The *Arabidopsis* DELAYED DEHISCENCE1 gene encodes an enzyme in the jasmonic acid synthesis pathway. Plant Cell **12:** 1041–1061

Schilmiller AL, Howe GA (2005) Systemic signaling in the wound response. Curr Opin Plant Biol **8:** 369–377

Schmidt S, Baldwin IT (2006) Systemin in *Solanum nigrum*: The tomato-homologous polypeptide does not mediate direct defense responses. Plant Physiol **142:** 1751–1758

Schmidt S, Baldwin IT (2009) Down-regulation of systemin after herbivory is associated with increased root allocation and competitive ability in *Solanum nigrum*. Oecologia **159:** 473–482

Sharma RK, Mazumder R (1970) Purification, properties, and feedback control of L-Threonine dehydratase from spinach. J Biol Chem **245:** 3008–3014

Sommer-Knudsen J, Bacic A, Clarke AE (1998) Hydroxyproline-rich plant glycoproteins. Phytochemistry **47:** 483–497

Stintzi A, Browse J (2000) The *Arabidopsis* male-sterile mutant, *opr3*, lacks the 12-oxophytodienoic acid reductase required for jasmonate synthesis. Proc Natl Acad Sci USA **97:** 10625–10630

Vanaltvorst AC, Bovy AG (1995) The role of ethylene in the senescence of carnation flowers, a review. Plant Growth Regul **16:** 43–53

von Dahl CC, Winz R, Halitschke R, Kühnemann F, Gase K, Baldwin IT (2007) Tuning the herbivore-induced ethylene burst: the role of transcripts accumulation and ethylene perception in *Nicotiana attenuata*. Plant J **51:** 293–307

Wang L, Halitschke R, Kang JH, Berg A, Harnisch F, Baldwin IT (2007) Independently silencing two members of the *JAR* family impairs levels of trypsin proteinase inhibitors but not nicotine. Planta **226:** 159–167

Whelan S, Goldman N (2001) A general empirical model of protein evolution derived from multiple protein families using a maximum-likelihood approach. Mol Biol Evol **18:** 691–699

Wu J, Hettenhausen C, Baldwin IT (2006) Evolution of proteinase inhibitor defenses in North American allopolyploid species of *Nicotiana*. Planta **224:** 750–760

Wu J, Hettenhausen C, Meldau S, Baldwin IT (2007) Herbivory rapidly activates MAPK signaling in attacked and unattacked leaf regions but not between leaves of *Nicotiana attenuata*. Plant Cell **19:** 1096–1122

Zavala JA, Patankar A, Gase K, Hui D, Baldwin IT (2004) Manipulation of endogenous trypsin proteinase inhibitor production in *Nicotiana attenuata* demonstrates their function as antiherbivore defenses. Plant Physiol **134:** 1181–1190